ANNUAL REVIEWS

Annual Review of Genomics and Human Genetics

Padlock Probe–Based Targeted In Situ Sequencing: Overview of Methods and Applications

Anastasia Magoulopoulou, Sergio Marco Salas, Katarína Tiklová, Erik Reinhold Samuelsson, Markus M. Hilscher, and Mats Nilsson

Department of Biochemistry and Biophysics, Science for Life Laboratory, Stockholm University, Solna, Sweden; email: anastasia.magoulopoulou@scilifelab.se, sergiomarco.salas@scilifelab.se, katarina.tiklova@scilifelab.se, erik.samuelsson@scilifelab.se, markus.hilscher@scilifelab.se, mats.nilsson@scilifelab.se

Annu. Rev. Genom. Hum. Genet. 2023. 24:133–50

First published as a Review in Advance on April 5, 2023

The *Annual Review of Genomics and Human Genetics* is online at genom.annualreviews.org

https://doi.org/10.1146/annurev-genom-102722-092013

Keywords

in situ sequencing, ISS, spatially resolved transcriptomics, SRT, rolling circle amplification, RCA, padlock probes, spatial cell atlas, in situ cell typing

Abstract

Elucidating spatiotemporal changes in gene expression has been an essential goal in studies of health, development, and disease. In the emerging field of spatially resolved transcriptomics, gene expression profiles are acquired with the tissue architecture maintained, sometimes at cellular resolution. This has allowed for the development of spatial cell atlases, studies of cell–cell interactions, and in situ cell typing. In this review, we focus on padlock probe–based in situ sequencing, which is a targeted spatially resolved transcriptomic method. We summarize recent methodological and computational tool developments and discuss key applications. We also discuss compatibility with other methods and integration with multiomic platforms for future applications.

INTRODUCTION

Organs and tissues consist of a variety of cells with specialized roles. A cell's environment can affect its function through gene expression regulation, often via external cues arising from local cell-to-cell communication. Deciphering tissue cellular composition and defining gene expression profiles in relation to function has been a continuous goal in biology. To understand physiology and disease, it is necessary to have the means of obtaining this information.

In recent years, the emergence of single-cell RNA sequencing (scRNA-seq) has enabled the high-throughput acquisition of cellular gene expression information (33, 59, 78, 96, 107). scRNA-seq has allowed the compartmentalization of tissue samples into their individual cellular components, the identification of differentially expressed genes at the cellular level, the identification of very rare cell types, and even the development of a paradigm of classifying cells (106). However, the technique requires tissue dissociation, which inevitably brings the loss of spatial context. Moreover, the experimental procedure itself can affect gene expression and consequently the identified transcriptional profile (82, 108). Additionally, scRNA-seq requires surviving intact cells, which leads to underrepresentation of sensitive or damaged cells (e.g., neurons with projecting axons outside of the excision area).

Spatially resolved transcriptomics (SRT), which *Nature Methods* named its Method of the Year in 2020 (63), connects transcriptomic data with spatial position within a tissue (4, 23, 50, 92), thus linking tissue architecture with the molecular signature of its cellular components. Cell type identification, spatial distribution of marker patterns, exploration of cell-to-cell interactions, and mapping of expression patterns in health, development, and disease are now possible at the regional, cellular, and subcellular levels (25). SRT is available via a wide range of technologies that are typically grouped in three main categories: (*a*) capture-based technologies coupled with next-generation sequencing, (*b*) image-based technologies based on sequential fluorescence in situ hybridization (FISH), and (*c*) image-based technologies based on signal amplification for in situ sequencing (ISS).

The first capture-based technology to be described was spatial transcriptomics (91), which uses slides that contain spots with barcoded oligonucleotides for mRNA capture and links all transcripts in a region with the region's coordinates. This technology provides transcriptome-wide coverage of the tissue content with no previous knowledge or data needed. Spatial transcriptomics was followed by 10x Visium (28, 39) and high-definition spatial transcriptomics (100), which provided higher definition with a smaller spot size. Similar technologies to spatial transcriptomics include Slide-seq (81) and Slide-seqV2 (62), which use DNA-barcoded beads for mRNA capture. Slide-seq offers transcriptome-wide coverage with low sensitivity, and Slide-seqV2 improves the assay's sensitivity to reach scRNA-seq sensitivity levels. The technologies that achieve simultaneous mRNA and protein capture are deterministic barcoding in tissue for spatial omics sequencing (DBiT-seq) (55), which uses a microfluidics barcode system, and spatial enhanced resolution omics sequencing (Stereo-seq) (16, 103), which uses DNA nanoballs for mRNA capture. Laser capture microdissection (17) combines single-cell-based PCR amplification and RNA-seq; this technique focuses on manually selected areas and offers low throughput with a resolution of 10 cells.

The challenges of capture-based techniques lie in their resolution, capture area, and capture efficiency, and each new version aims to improve these aspects. Additionally, applying these methods requires consideration of the cost and required expertise as well as the computational needs for data analysis.

The second category is image-based technologies based on sequential FISH. In situ hybridization technologies offer sensitive detection of mRNA molecules with subcellular resolution and various grades of multiplexing depending on the applied technologies. Amplified single-molecule FISH (smFISH) (86) with the use of single-molecule hybridization chain reaction (smHCR)

offers high sensitivity with limited throughput. Ouroboros smFISH (osmFISH) (22), which was commercialized by Rebus Biosystems, detected 33 transcripts in mouse brain. Multiplexed error-robust FISH (MERFISH) (18), which was commercialized by Vizgen as MERSCOPE, achieved a throughput of approximately 150 RNA transcripts (18, 65) when combined with error identification and correction. SeqFISH with the use of combinatorial decoding (86) increased throughput from 32 mRNA transcripts to 10,000 when confocal microscopy was used in place of super-resolution microscopy and pseudocoloring decoding schemes were introduced for multiplexing (27, 57).

FISH-based technologies often need to be combined with tissue clearing due to tissue autofluorescence. They also rely on high magnification microscopy, which increases the imaging time and decreases the scanning area size.

Finally, in this review we focus on the third category, advances in image-based technologies based on signal amplification with the use of padlock probes for ISS; we present applications of this technology in order to discuss the enabling features of these applications. Many image-based technologies are based on signal amplification for ISS. Variants include gap-filled ISS, which is used to measure the sequence of short portions of the targeted RNA (41), and spatially resolved transcript amplicon readout mapping (STARmap), which uses specific amplification of nucleic acids via intramolecular ligation (SNAIL) probes (102). Untargeted ISS methods include fluorescence ISS (FISSEQ) (48, 49). Other modifications include targeted expansion sequencing (ExSeq), which uses expansion microscopy and long-read in situ RNA sequencing (2); barcoded anatomy resolved by sequencing (BARSeq) (21); and BARSeq2 (94).

IN SITU SEQUENCING

ISS, as originally described by Ke et al. (41), identifies mRNA molecules in tissues in multiplex fashion with the use of padlock probes (see **Figure 1**). Padlock probes are linear oligonucleotides approximately 70 nt in length, consisting of a customizable backbone and two 20-nt-long arms that are complementary to the target sequence (69). The backbone includes a target-transcript-specific barcode sequence and a general identification sequence called the anchor sequence. Upon fixation and permeabilization of the tissue specimen, the mRNA is reverse transcribed to cDNA and then degraded with the use of RNase H. The padlock probes are then hybridized to the cDNA, and the nick between the two probe arms in juxtaposition is sealed by *Thermus thermophilus* DNA ligase. This ligase catalyzes the formation of phosphodiester bonds between adjacent 3′-hydroxyl and 5′-phosphate termini in double-stranded DNA in a NAD-dependent manner.

The ISS method's main assets are its high thermostability, which allows for the use of stringent hybridization conditions, and its highly discriminative activity toward nonperfect matches. *Thermus thermophilus* DNA ligase can discriminate even single mismatches at the 3′ end of the padlock probe, thus allowing for high specificity and the identification of single-nucleotide polymorphisms (30, 44, 58, 98). The created DNA circle is amplified by target-primed rolling circle amplification with the use of φ29 polymerase, resulting in a single-stranded rolling circle product (RCP) that contains hundreds of copies of the circularized padlock probe and spatially collapses in submicron-sized blobs, sometimes referred to as DNA nanoballs or rolling circle colonies (rolonies).

As described in Ke et al. (41), the generated RCP is subjected to sequencing by ligation, where a fluorophore-conjugated anchor primer is hybridized to the general identification sequence copies in the RCP, right next to the fluorophore-conjugated interrogation probes that are specific for each unique transcript barcode. The interrogation probes consist of four libraries of 9-mers with one fixed position (A, T, G, or C) and eight random positions (N). Upon hybridization of the anchor primer, the interrogation probe with the best base match for the examined barcode position is

incorporated by ligation and displays the color that corresponds to the matched base. This allows for the specific detection of gene signals upon decoding and reduces the likelihood of off-target probe specificity.

After the rolling circle amplification step, the anchor and barcode sequences of the padlock probe backbone are amplified hundreds of times, allowing for multiple bindings of the anchor primer and interrogation probes for every single target molecule. This leads to an amplified fluorescence signal and decreased signal-to-noise ratio, enabling the use of lower magnification objectives to resolve signals, which in turn enables the scanning of large areas and reduces imaging time. After each imaging cycle, the anchor and interrogation probes can be stripped and washed away. These steps are then repeated with the interrogation probe libraries of the next barcode base. Barcode decoding is done by using further image analysis to identify the fluorescence patterns across the sequencing cycles, a process that is discussed in further detail below (see the section titled Increased Multiplexity). For a step-by-step protocol of the first-generation ISS chemistry, we direct readers to Reference 35.

METHODOLOGICAL ADVANCES OF IN SITU SEQUENCING

Increased Multiplexity

ISS was first used to distinguish 39 RNAs in breast cancer slices (41). Gyllborg et al. (32) further developed ISS by both introducing a new barcoding system and replacing the sequencing-by-ligation reaction chemistry with hybridization-based ISS (HybISS) for detection (see **Figure 1**). The first-generation ISS method uses a four-base barcode on the padlock probe backbone for transcript identification, which is enough to decode $4^4 = 256$ different transcripts. In HybISS, the padlock probes have two target complementary arms at their 3′ and 5′ ends, and the probe

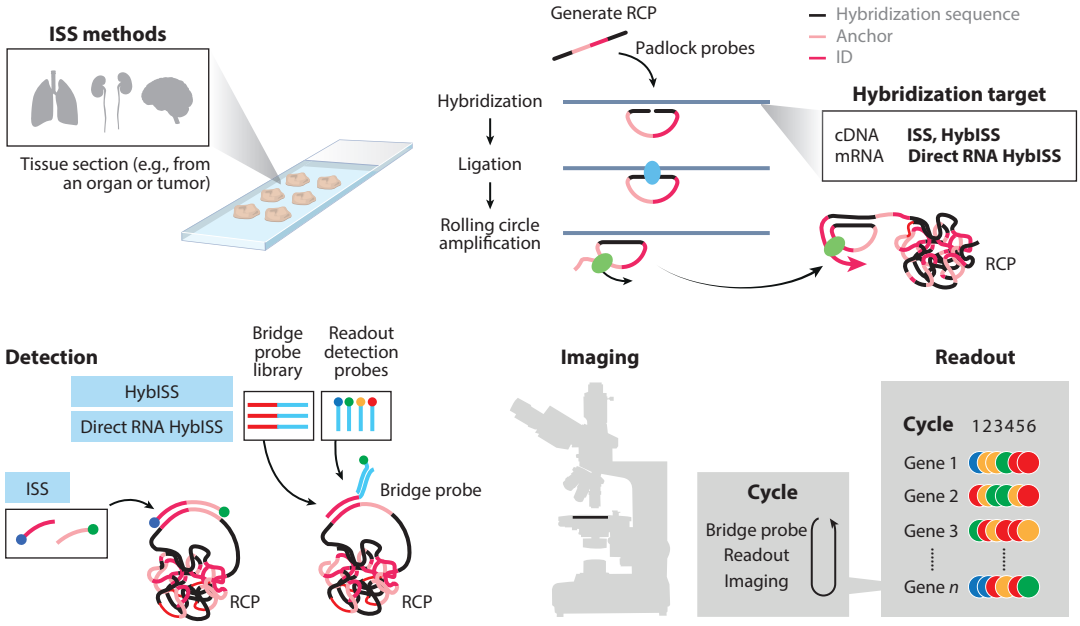

Figure 1

Principal workflow of ISS, highlighting the main differences among ISS, HybISS, and direct RNA HybISS. Abbreviations: HybISS, hybridization-based in situ sequencing; ISS, in situ sequencing; RCP, rolling circle product.

Table 1 Comparison of ISS, HybISS, and direct RNA HybISS methodologies

Method	Target	Detection	Readout	Original publication
ISS	Reverse-transcribed mRNA (cDNA) ~1% efficiency	Sequencing by ligation Anchor and detection probes	Up to 256 transcripts Barcode decoding Single-nucleotide discrimination	41
HybISS	Reverse-transcribed mRNA (cDNA) ~1% efficiency	Sequencing by hybridization L-probes and detection probes	Theoretically unlimited number of transcripts Potential optical crowding Flexible decoding scheme Increased signal intensity Increased signal-to-noise ratio Suitable for autofluorescent tissues Single-nucleotide discrimination	32
Direct RNA HybISS	mRNA Up to 5% efficiency	Sequencing by hybridization L-probes and detection probes	Theoretically unlimited number of transcripts Potential optical crowding Flexible decoding scheme Increased signal intensity Increased signal-to-noise ratio Suitable for autofluorescent tissues	47

Abbreviations: HybISS, hybridization-based in situ sequencing; ISS, in situ sequencing.

backbone comprises a common anchor sequence and a 20-nt ID sequence that is unique for every target transcript. For the detection step, HybISS uses sequential hybridization of libraries of L-probes (also known as bridge probes) and fluorescently labeled detection probes (see **Table 1**). The L-probes are 40 nt long, with a 17-nt sequence that recognizes the ID sequence of each target transcript, a 3-nt linker, and a 20-nt sequence where the fluorescently labeled detection oligonucleotides will bind. The 17-nt part that recognizes the ID sequence remains constant between the L-probe libraries that identify the same transcript among the different imaging cycles, whereas the 20-nt sequence for the detection oligonucleotide differs between the L-probe libraries of every imaging cycle according to the given transcript barcode (32).

The HybISS design allows for increased flexibility and multiplexing, overcoming the 256-transcript limit to allow for a theoretically unlimited number of detected transcripts. The challenge in transcript detection here is the optical crowding of signals, which can be addressed with adjusted imaging and decoding schemes (47). Moreover, since HybISS uses hybridization instead of ligation for the detection of fluorescent signals, it is not limited by the efficiency of the ligation. Consequently, a larger number of L-probes and detection oligonucleotides are hybridized in every RCP, giving a higher signal intensity as well as an improved signal-to-noise ratio.

Increased Detection Efficiency

After the commercialization of ISS in 2018 by CARTANA (34), the method was further developed to directly target mRNA molecules with the use of chimeric padlock probes (42). This approach skips the reverse transcription step and the subsequent fixation of the newly synthesized cDNA, which (along with the other enzymatic steps) contribute to the comparatively low efficiency of the ISS method (41). By skipping the reverse transcription step and directly targeting the RNA, the method achieves a fivefold increase in the efficiency of in situ detection of individual transcripts while maintaining specificity, throughput, and multiplexing (38, 47) (**Figure 1**; **Table 1**).

Single-cell-resolution in situ hybridization on tissues (SCRINSHOT) (89) and barcoded oligonucleotides ligated on RNA amplified for multiplexed and parallel in situ analyses (BOLORAMIS) (54) are versions of ISS with direct hybridization of padlock probes on mRNA. **Table 2** compares a variety of studies that applied padlock probe–based technology (ISS, HybISS, or SCRINSHOT).

COMPUTATIONAL METHODS

The image-based nature of SRT technologies that use rolling circle amplification leads to nontrivial processing, decoding, and analysis requirements for the data generated by these methods. The assembly of individual fields of view into single large images of the tissues (via stitching) and the fine alignment of the different imaging rounds generated by SRT methods (image registration) represent the first computational challenge in the processing of SRT data. A recently developed tool, Alignment by Simultaneous Harmonization of Layer/Adjacency Registration (ASHLAR), allows coordinated stitching and registration, which guarantees an improved alignment of the different rounds through the entire imaged tissue (66).

Decoding—the detection and identification of the RCP's identity—is one of the most challenging steps in the processing of SRT datasets, mostly due to optical crowding and tissue autofluorescence, leading to difficulty identifying gene signals. Recently developed decoding algorithms, such as In Situ Transcriptomics Decoding by Deconvolution (ISTDECO) (3), Barcode Demixing Through Non-Negative Spatial Regression (BarDensr) (19), and PoSTcode (31), have addressed this issue by spatially deconvolving the expression of every expected gene, generating one deconvolved image for every gene and facilitating the identification of signals on these images, and allowing the resolution of normally difficult-to-identify signals. These algorithms reported an improved identification of signals, especially in optically crowded areas. Graph-based approaches (74) have also shown their potential in the decoding of optically crowded regions.

Most applications of SRT rely on the identification of cells in the tissue, which requires assigning decoded RCPs to cells. Usually, a nuclear stain [e.g., 4′,6-diamidino-2-phenylindole (DAPI)] is imaged together with the imaging cycles and used as a reference to place cell nuclei. The segmentation of these nuclei, though, can be a complex task, especially in densely packed tissues using classical watershed algorithms. Recently, deep learning models such as Cellpose (93), ilastik (10), and StarDist (85) have been proven to outperform the gold standard segmentation methods and are starting to be widely used to segment cells in image-based SRT (46, 101). Despite the improvements, however, nuclear segmentation is far from perfect, since it fails to segment the entire cell bodies. As a consequence, RCPs located in cells' cytoplasm can typically be lost or misassigned. To overcome this problem, nuclei-free segmentation methods, such as Baysor (77) and spot-based spatial cell type analysis by multidimensional mRNA density estimation (SSAM) (72), rely on RCPs' density and identity to segment individual cells. In densely packed tissues, where density-based segmentation can be challenging, Baysor can be complemented with nuclear-based segmentation for improved cellular segmentation. To address the same issue, spage2vec (75), a graph-based algorithm, has proven able to recapitulate local gene expression patterns solely relying on the subcellular context of each RCP without the need of any type of segmentation.

The main objective of segmenting individual cells is to decipher their molecular identity. A common strategy for identifying cell populations is to use scRNA-seq analysis packages, such as Scanpy or Seurat, to perform de novo clustering. However, this task can be challenging in some datasets, mainly due to the reduced number of genes used in the panel and the low number of reads per cell detected in the experiments. An alternative to de novo clustering is to identify cell populations by matching the SRT data with scRNA-seq (1, 11), allowing the user to impute the expression of genes not present in the panel. Some of these algorithms, such as probabilistic cell

Table 2 Overview of studies in mouse and human that used padlock probe–based technology (ISS, HybISS, or SCRINSHOT), with details on tissue types, cell types studied, and number of target genes

Study	Tissue type(s) used	Species	Main cell type(s) studied	Number of target genes	Method(s) used	Application/novelty of spatial approach
Ke et al. (41)	Breast cancer	Human	Cancer cells and fibroblast cells	39	ISS	Development of ISS method
Soldatov et al. (87)	Neural crest	Mouse	Trunk and cranial neural crest cells	32	ISS	Investigation of spatiotemporal dynamics associated with early cell fate decisions in mouse trunk and cranial neural crest cells
Tiklová et al. (97)	Midbrain	Mouse	Neuronal cells	49	ISS	Transcriptomic mapping of midbrain dopamine neuron maturation
Carow et al. (15)	Lung	Mouse	Cells in tuberculosis granuloma	34	ISS	Comparison of *Mycobacterium tuberculosis* granulomas in lungs from mice
Asp et al. (5)	Heart	Human	Cardiac cells	69	ISS, ST	Mapping of the human developing heart
Qian et al. (79)	Hippocampus and isocortex	Mouse	Neuronal cells	99	ISS, pciSeq	Introduction of pciSeq and mapping of the inhibitory neurons of mouse hippocampal area CA1
Chen et al. (20)	Isocortex	Mouse and human	Neurons, astrocytes, oligodendrocytes, microglia	84	ISS, ST	Investigation of the pathology of Alzheimer's disease at a genome-wide scale
Sountoulidis et al. (88)	Lung, kidney, and heart	Mouse and human	Many different cell types	147	SCRINSHOT	Direct hybridization of padlock probes on mRNA and mapping of the locations of abundant and rare cell types
Langseth et al. (45)	Brain	Human	Neuronal and nonneuronal cells	120	HybISS, pciSeq	Creation of the first spatial atlas of human cortical cells
La Manno et al. (43)	Brain	Mouse	Neuronal and nonneuronal cells	119	HybISS, smFISH	Creation of a transcriptomic atlas of the embryonic mouse brain between gastrulation and birth

(*Continued*)

Table 2 (*Continued*)

Study	Tissue type(s) used	Species	Main cell type(s) studied	Number of target genes	Method(s) used	Application/novelty of spatial approach
Hilscher et al. (36)	Isocortex, corpus callosum, and spinal cord	Mouse	Oligodendrocytes	124	ISS, pciSeq	Creation of a transcriptomic atlas of fine oligodendrocyte subtypes
Van Bruggen et al. (99)	Forebrain	Human	Oligodendrocytes	50	HybISS, pciSeq	Mapping of the neural diversity in the human forebrain at postconception weeks 8–10
Sountoulidis et al. (89)	Lung	Human	Lung cells	31 + 146	HybISS, SCRINSHOT, pciSeq	Creation of a topographic atlas of early human lung development
Magoulopoulou et al. (60)	Lung	Mouse	Cells in tuberculosis granuloma	36	ISS	In-depth study of immune cells interacting with *Mycobacterium tuberculosis* in the infected lung tissue

Abbreviations: HybISS, hybridization-based in situ sequencing; ISS, in situ sequencing; pciSeq, probabilistic cell typing by in situ sequencing; SCRINSHOT, single-cell-resolution in situ hybridization on tissues; smFISH, single-molecule fluorescence in situ hybridization; ST, spatial transcriptomics.

typing by ISS (pciSeq) (79), combine cell type identification with segmentation, assigning reads to cells depending on the identity of the cells themselves.

The main advantage of SRT approaches is their ability to generate single-cell-resolution maps of cell types. Although visual inspection of the maps is useful to understand the structure of the analyzed tissues, some deeper spatial statistics are necessary to further understand the data. Several packages [Squidpy (71a), Giotto (25a), Seurat (32a, 84a), and Matisse (83a)] have been developed for this purpose, allowing the exploration of the spatial architecture of tissues. In addition, new tools to identify tissue domains [e.g., BANKSY (86a)], explore cell–cell communication (node-centric expression models), or even uncover subcellular patterns within cells [Bento (60a)] are rapidly emerging and promise to bring the analysis of SRT datasets to the next level.

EFFORTS TO GENERATE CELL ATLASES: FOCUS ON IN SITU SEQUENCING

Due to the vast number and complexity of tissues—the central nervous system alone consists of more than 80 billion postmitotic neurons (7, 76)—high-throughput methods are needed to screen as many cells in as short a time as possible. scRNA-seq can investigate single-cell RNA, assessing up to 20,000 individual cells simultaneously with high sensitivity (51), and comprehensive molecular databases are currently being generated within large community efforts. Since biological functions are performed via the concerted activities of many different cell types interacting in a three-dimensional environment, scRNA-seq efforts can then be combined with spatial transcriptomics methods to pinpoint the exact locations of the studied cells. The Human Cell Atlas

community effort aims to create a consensus molecular taxonomy and cell atlases for all organs in the human body (52, 80). The Brain Research Through Advancing Innovative Neurotechnologies (BRAIN) Initiative cell census effort has the goal of creating high-resolution whole-brain cell type atlases for mice, humans, and nonhuman primates (26, 67, 68). With a cross-species consensus molecular taxonomy of cell types in place, cellular organization can now be comprehensively mapped (4, 14, 92). And even tissue compartmentalization, such as automated identifications of brain regions or reference mappings, are possible with SRT data (12, 71, 73).

ISS efforts to generate cell atlases include the profiling of hundreds of RNAs in mouse tissues, including midbrain (97), neural crest (87), hippocampus (79), cortex (20), corpus callosum (29, 36), spinal cord (29, 36), developing mouse brain (43), and kidney (88). Most recently, zebrafish heart tissue samples have also been mapped (90). Regarding human tissues, studies have applied ISS to adult brain tissue sections (45), forebrain (99), and developing lung and heart tissues (5, 89); in these studies, pciSeq has been applied to assign detected transcripts to segmented cells and, subsequently, cells to cell types (79). This approach allows a straightforward integration of spatial data with a consensus molecular taxonomy, such as the Human Cell Atlas or the BRAIN Initiative Cell Census Network.

In the following sections, we focus on some of the highlights of the ISS studies and discuss their integration with previous knowledge in the fields of neurobiology and cancer research as well as further applications to disease (see graphical summary in **Figure 2**).

NEUROBIOLOGY: INSIGHTS FROM PADLOCK PROBE–BASED METHODS

One of the first ISS studies focused on neuronal cell types by combining scRNA-seq and ISS to study midbrain dopamine neuron diversity (97). Unraveling the diversity of dopamine neurons is necessary to gain a better understanding of why only certain subtypes degenerate in Parkinson's disease. Tiklová et al. (97) performed scRNA-seq of isolated neurons expressing transcription factor Pitx3, a marker for dopamine neurons, which identified seven subgroups with

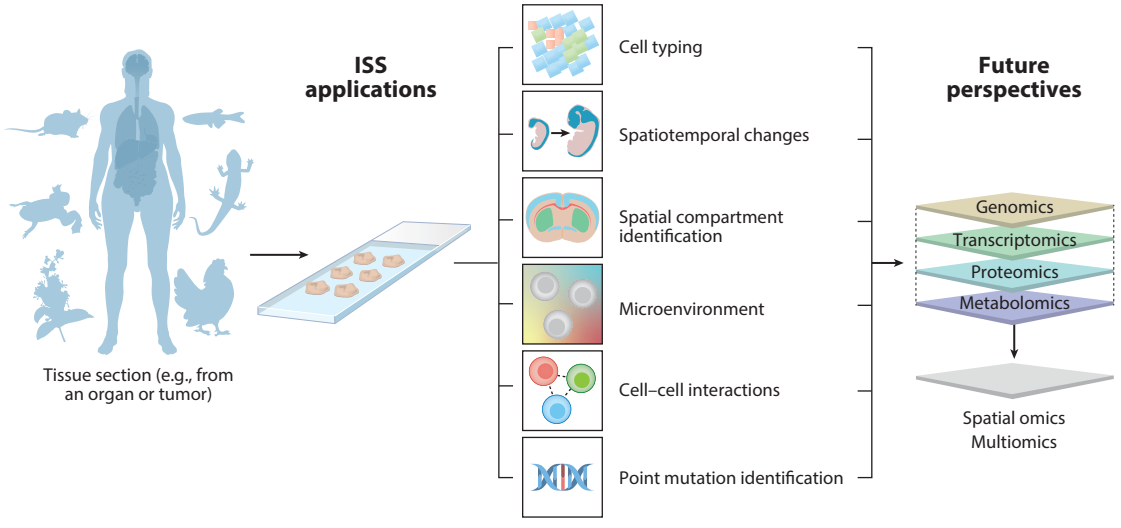

Figure 2

Tissues, species, and applications of padlock probe–based ISS technologies. Abbreviation: ISS, in situ sequencing.

this subtype-specific marker. To localize the seven identified subgroups, they used a combination of subgroup-distinguishing markers identified via classical histological methods and ISS. The classical histological methods mapped each subgroup separately by combining 3 genes at a time, whereas the ISS method used 49 genes and simultaneously localized all seven subgroups at the single-cell level. ISS was also used to quantify the proportion of cells per subgroup, revealing that specific subgroups are significantly underrepresented in the scRNA-seq data. The strategy to combine scRNA-seq and ISS provided a powerful resource for studies of midbrain dopamine neurons. Furthermore, identification of specific subtypes enabled more focused research into Parkinson's disease etiology and the generation of desired subtypes for regenerative medicine.

La Manno et al. (43) focused on mouse brain development between gastrulation and birth by combining extensive droplet-based single-cell sequencing and ISS. Single-cell sequencing identified almost 800 cellular states (as defined by dimensionally reduced clusters), divided into 25 categories. The developing brain consists of spatial domains characterized by expression of specific transcription factors. To link the spatial domains and transcriptional cell state, the authors performed ISS using 119 genes identified by single-cell sequencing. ISS mapped many clusters but also mapped spatial variability within the clusters. Combining those two powerful techniques provided time-, lineage-, and region-specific gene expression profiles, which are important for advancing the understanding of brain and neurological disorder development.

ISS has also been used to characterize the spatial and temporal heterogeneity of oligodendrocyte subtypes in both mice and humans. Oligodendrocytes arise during embryonic development in different waves. Their function is to support and isolate axons through the myelin production. Hilscher et al. (36) used ISS to profile 124 marker genes that distinguish 12 previously characterized oligodendrocyte populations. They performed ISS analysis on three regions of the juvenile and adult mouse central nervous system. The results extended previous findings by profiling the detailed spatial organization of oligodendrocyte lineage populations. Using a panel for genes specific for different developmental stages uncovered the timing of oligodendrocyte differentiation and myelination in specific areas.

In another study, van Bruggen et al. (99) focused on human oligodendrogenesis and profiled human fetal forebrain to identify the ventral sites where oligodendrogenesis occurs first. To start, they combined single-cell transcriptomics with a single-cell assay for transposase-accessible chromatin using sequencing (scATAC-seq) and found that human forebrain contains cells with chromatin states compatible with oligodendrogenesis at the first trimester. To determine the exact location of those cells, they selected 50 genes identified by scRNA-seq and scATAC-seq for ISS analysis. The combination of all those methods resulted in a comprehensive study that gives a more complete picture of oligodendrogenesis. There are several demyelinating disorders, such as multiple sclerosis, where a deep understanding of oligodendrogenesis and myelin formation is crucial for modulation of myelin repair, and this work helps advance the understanding of the fundamental mechanisms of such disorders.

UNDERSTANDING CANCER USING IN SITU SEQUENCING

With the advent of scRNA-seq as a ubiquitous tool in profiling the cells that make up cancer comes the need to determine how the same cells organize themselves in their native context. By selecting biomarkers defined by literature, bulk RNA studies, or scRNA-seq studies, one can create customized probe panels and validate the expression of those biomarkers in patient tissue to identify disease mechanisms associated with tumor microenvironments, phenotypes, and disease mechanisms. Most importantly, SRT can be used to profile not only the organization of cells in the tumor microenvironment but also the inherent complexity of the disease. Cancers are assemblies of heterogeneous populations of various distinct cell types, genetic compositions, and phenotypes,

and their variability can complicate our ability to assign definite identities to cells. To disentangle the complex network of interactions in cancer is an ongoing struggle, one that can be successfully done with the right tools.

To give an example, Liu et al. (53) profiled the structure of diffuse midline gliomas, a class of glioma defined by the K27M mutation in histone H3. To chart scRNA-seq/single-nucleus ATAC-seq–derived tumor cell subpopulations within the intact tissue architecture of H3 K27M diffuse midline gliomas, the authors used the SRT approach of HybISS (32). Using combinatorial marker genes specific for individual malignant and nonmalignant cell types from tumor scRNA-seq and published normal brain scRNA-seq datasets, they generated padlock probes to create a panel of 130 curated marker genes. They then used probabilistic cell typing via pciSeq (79), complemented by immunofluorescence staining against the K27M mutation within the same tissue sections, to confidently identify both malignant and nonmalignant cell types, as well as individual tumor cell populations, thereby resolving the single-cell spatial architectures of 16 primary patient H3 K27M diffuse midline gliomas spanning different age groups and locations.

In another case, Ruiz-Moreno et al. (83) investigated the spatial architecture of two glioblastoma tissues using generated padlock probes against 194 genes specific for malignant (oligodendrocyte precursor cell–like, astrocyte cell–like, neural precursor cell–like, and mesenchymal cell–like) and nonmalignant cells (microglia, macrophages, oligodendrocytes, astrocytes, neurons, endothelial cells, T cells, dendritic cells, and mural cells), as well as signaling markers of interest. The cell types that compose the glioblastoma tumor microenvironment were mapped and assigned transcripts to cells through pciSeq (79). Notably, the glioblastoma malignant cells showed a layered distribution around the endothelial and mural cells. These results indicate that not only were all malignant phenotypes present in sections and engaged in specific activities by type, but they were each localized in a preferred nonmalignant niche.

The spatial transcriptomic portions of both the glioblastoma study (83) and the diffuse midline glioma study (53) established not only that there is significant diversity in cell composition between tumors, but also that HybISS (*a*) identifies true cell state proportions, in contrast to scRNA-seq, and (*b*) identifies cell states not seen in scRNA-seq datasets, by including genes for cell states that were expected but not present in the scRNA-seq dataset (neurons, pericytes, etc.). Furthermore, these studies found that cancer cell phenotypes and nonmalignant phenotypes exhibit specific spatial distribution patterns, shedding light on local cellular relationships and niches between individual malignant populations as well as between malignant and nonmalignant populations.

An additional area of application of SRT that is of importance in cancer research is plotting cancer evolution. Cancer cells evolve through rounds of mutation and selection and become more evolutionarily fit and resistant to treatment (13, 64, 70). As a result of the repeated process of mutation and selection, cancers are patchworks of genetically related but distinct groups of cells, termed subclones (24). This is not a trend confined to individual types of cancer; as seen by the Tracking Cancer Evolution Through Therapy (TRACERx) project, even the smallest cancers are miniature patchwork blankets stitched together from even smaller clones of genetically different cells (8). More importantly, mapping clonal evolution has particular relevance to patient cancer progression and the development of treatment; further studies have found that the same patterns of genetically distinct subclones contribute to the progression, growth, and recurrence of breast cancer (104, 105), esophageal adenocarcinoma (61), and non-small-cell lung cancer (37).

To generate molecular maps of breast cancer, Svedlund et al. (95) used a panel of 91 ISS padlock probes, consisting of breast cancer prognostic and predictive markers and cellular pathway–related genes, to create ISS-based OncoMaps that linked tumor histology and molecular signatures. These OncoMaps revealed intratumoral subtypes based on marker expressions such as Ki-67 or estrogen receptor, highlighting the prognostic importance of intratumoral heterogeneity. Building off of

this work, Lomakin et al. (56) developed base-specific ISS (BaSISS), an extension of the ISS protocol that incorporates multiplexed detection of clone-specific mutations in breast cancer patient biopsy sections, to map the distribution of mutant gene transcripts that denote specific subclones in these sections. BaSISS can be used to assess how patterns of spatial genetic heterogeneity can be influenced by resident tissue structures, how coexistent genetic clones can have distinct characteristics, and which local tumor microenvironments play host to specific subclones. Recently, stage II colon cancer patient samples have also been examined by ISS, and the neoplastic and non-neoplastic compartments could be successfully distinguished based on the spatial expression patterns obtained (84).

CHARACTERIZING DISEASE USING IN SITU SEQUENCING

To break down tissues into their localized molecular components and understand normal function and disease, efforts have been made to connect transcriptomic data to the morphological characteristics of the examined tissues.

Carow et al. (15) performed histopathology-driven analysis of *Mycobacterium tuberculosis* (Mtb)–infected mouse lungs based on hematoxylin and eosin staining and ISS data in order to directly compare uninfected and Mtb-infected lung areas. Additionally, compartmentalization of histological features of organized and non-organized granulomas (a tuberculosis disease hallmark) by manual area selection revealed distinct transcriptional signatures of immune markers. Since in tuberculosis the bacterial presence is leading the immune response and the subsequent histological changes, the expression of immune markers in relation to Mtb localization has been examined in relation to the localization of single bacteria (15, 60) and bacterial clusters (60). For this purpose, after the ISS protocol, the same tissues were stained for Mtb with auramine–rhodamine T staining, and the coordinates of the fluorescent signals were associated with ISS data coordinates (15, 60) in relation to their distance from the identified bacteria or clusters. The analysis showed differences in the composition of the immune microenvironment in each lesion type. In C57BL/6 mouse lungs, markers associated with macrophages and macrophage activation were enriched in subcellular distances to bacteria over time. However, no distinct spatial distribution of T cell responses was observed. In C3HeB/FeJ mouse lungs, small bacterial clusters were enriched for transcripts such as *Cd68* and *Inos*, whereas organized granulomas showed enrichment for *Cd8a*, *Tcrb*, and *Foxp3*. Since all the experimental procedures (ISS, auramine–rhodamine T staining, and hematoxylin and eosin staining) were conducted on the same tissue specimen, it was possible to acquire the exact tissue coordinates for every method. The same analysis can be performed to link ISS data to immunohistochemical signals of marker expression as long as the same slide is used for both experiments in order to acquire the exact coordinates.

SRT also provides a novel approach to untangle the cellular network in the vicinity of cells affected by diseases like Alzheimer's disease. A fundamental question in Alzheimer's disease is the relationship between amyloid plaques and the surrounding cells, as well as their role as a trigger of the neurodegeneration process (40). ISS enables the characterization of the transcriptomic profile of both diseased and healthy cells in their native context. Chen et al. (20) used two spatial methods, ISS and spatial transcriptomics, to demonstrate that amyloid plaques have a clear effect on all cell types in the amyloid plaque niche. Spatial transcriptomics revealed transcriptional changes early in Alzheimer's disease development in a coexpression network enriched for myelin and oligodendrocytes and in late-stage Alzheimer's disease development in a coexpression network enriched for plaque-inducing genes. These results were confirmed by ISS as well as by single-cell-level gene expression analysis and by the investigation of gene expression around the formed plaques in 100-μm rings (20). Overlay of immunostaining, DAPI, selections of cells, and plaque images was

facilitated with image analysis tools such as QuPath (9). Those analyses provide a unique approach to characterize the regions with pathogenic hallmarks and how the spread of the pathology affects the neighboring cells in a non-cell-autonomous way.

CHALLENGES, LIMITATIONS, AND FUTURE DIRECTIONS

Work in this field has until now been done using in-house-developed reagents, imaging, and image analysis solutions, which has led to challenges for laboratories in applying these methods and in how to share and compare data. The coming years will see generations of fully automated commercial SRT systems facilitating standardization and broader implementation of this set of technologies. It is unlikely that there will be one dominating SRT system, as was the case for Illumina's next-generation sequencing instrumentation, so global efforts toward the standardization of the processing pipelines available for image-based SRT, such as the starfish initiative (6), are still very much needed. Given that this technology is still at an early stage of maturity, it is also quite likely that there will still be room for homemade solutions that test and provide analytical capabilities not yet implemented in the commercial systems. We can expect to see innovations that provide higher throughput at a lower cost, generate multiomic data, and produce three-dimensional data for creating multimodal atlases and beyond.

DISCLOSURE STATEMENT

M.N. is an advisor for the company 10x Genomics.

ACKNOWLEDGMENTS

We thank Mattias Karlen for creating the illustrations used for the figures in this review.

LITERATURE CITED

1. Abdelaal T, Mourragui S, Mahfouz A, Reinders MJT. 2020. SpaGE: Spatial Gene Enhancement using scRNA-seq. *Nucleic Acids Res.* 48:e107
2. Alon S, Goodwin DR, Sinha A, Wassie AT, Chen F, et al. 2021. Expansion sequencing: spatially precise in situ transcriptomics in intact biological systems. *Science* 371:eaax2656
3. Andersson A, Diego F, Hamprecht FA, Wählby C. 2021. ISTDECO: In Situ Transcriptomics Decoding by Deconvolution. bioRxiv 2021.03.01.433040. **https://doi.org/10.1101/2021.03.01.433040**
4. Asp M, Bergenstråhle J, Lundeberg J. 2020. Spatially resolved transcriptomes—next generation tools for tissue exploration. *BioEssays* 42:1900221
5. Asp M, Giacomello S, Larsson L, Wu C, Fürth D, et al. 2019. A spatiotemporal organ-wide gene expression and cell atlas of the developing human heart. *Cell* 179:1647–60.e19
6. Axelrod S, Cai M, Carr AJ, Freeman J, Ganguli D, et al. 2021. starfish: scalable pipelines for image-based transcriptomics. *J. Open Source Softw.* 6:2440
7. Azevedo FAC, Carvalho LRB, Grinberg LT, Farfel JM, Ferretti REL, et al. 2009. Equal numbers of neuronal and nonneuronal cells make the human brain an isometrically scaled-up primate brain. *J. Comp. Neurol.* 513:532–41
8. Bailey C, Black JRM, Reading JL, Litchfield K, Turajlic S, et al. 2021. Tracking cancer evolution through the disease course. *Cancer Discov.* 11:916–32
9. Bankhead P, Loughrey MB, Fernández JA, Dombrowski Y, McArt DG, et al. 2017. QuPath: open source software for digital pathology image analysis. *Sci. Rep.* 7:16878
10. Berg S, Kutra D, Kroeger T, Straehle CN, Kausler BX, et al. 2019. Ilastik: interactive machine learning for (bio)image analysis. *Nat. Methods* 16:1226–32
11. Biancalani T, Scalia G, Buffoni L, Avasthi R, Lu Z, et al. 2021. Deep learning and alignment of spatially resolved single-cell transcriptomes with Tangram. *Nat. Methods* 18:1352–62

12. Borm LE, Mossi Albiach A, Mannens CCA, Janusauskas J, Özgün C, et al. 2023. Scalable in situ single-cell profiling by electrophoretic capture of mRNA using EEL FISH. *Nat. Biotechnol.* 41:22–31
13. Cairns J. 1975. Mutation selection and the natural history of cancer. *Nature* 255:197–200
14. Callaway EM, Dong H-W, Ecker JR, Hawrylycz MJ, Huang ZJ, et al. 2021. A multimodal cell census and atlas of the mammalian primary motor cortex. *Nature* 598:86–102
15. Carow B, Hauling T, Qian X, Kramnik I, Nilsson M, Rottenberg ME. 2019. Spatial and temporal localization of immune transcripts defines hallmarks and diversity in the tuberculosis granuloma. *Nat. Commun.* 10:1823
16. Chen A, Liao S, Cheng M, Ma K, Wu L, et al. 2022. Spatiotemporal transcriptomic atlas of mouse organogenesis using DNA nanoball-patterned arrays. *Cell* 185:1777–92.e21
17. Chen J, Suo S, Tam PP, Han J-DJ, Peng G, Jing N. 2017. Spatial transcriptomic analysis of cryosectioned tissue samples with Geo-seq. *Nat. Protoc.* 12:566–80
18. Chen KH, Boettiger AN, Moffitt JR, Wang S, Zhuang X. 2015. Spatially resolved, highly multiplexed RNA profiling in single cells. *Science* 348:aaa6090
19. Chen S, Loper J, Chen X, Vaughan A, Zador AM, Paninski L. 2021. BARcode DEmixing through Non-negative Spatial Regression (BarDensr). *PLOS Comput. Biol.* 17:e1008256
20. Chen W-T, Lu A, Craessaerts K, Pavie B, Sala Frigerio C, et al. 2020. Spatial transcriptomics and in situ sequencing to study Alzheimer's disease. *Cell* 182:976–91.e19
21. Chen X, Sun Y-C, Zhan H, Kebschull JM, Fischer S, et al. 2019. High-throughput mapping of long-range neuronal projection using in situ sequencing. *Cell* 179:772–86.e19
22. Codeluppi S, Borm LE, Zeisel A, La Manno G, van Lunteren JA, et al. 2018. Spatial organization of the somatosensory cortex revealed by osmFISH. *Nat. Methods* 15:932–35
23. Crosetto N, Bienko M, van Oudenaarden A. 2015. Spatially resolved transcriptomics and beyond. *Nat. Rev. Genet.* 16:57–66
24. Dentro SC, Leshchiner I, Haase K, Tarabichi M, Wintersinger J, et al. 2021. Characterizing genetic intra-tumor heterogeneity across 2,658 human cancer genomes. *Cell* 184:2239–54.e39
25. Dries R, Chen J, del Rossi N, Khan MM, Sistig A, Yuan G-C. 2021. Advances in spatial transcriptomic data analysis. *Genome Res.* 31:1706–18

25a. Dries R, Zhu Q, Dong R, Eng C-HL, Li H, et al. 2021. Giotto: a toolbox for integrative analysis and visualization of spatial expression data. *Genome Biol.* 22:78

26. Ecker S, Chen L, Pancaldi V, Bagger FO, Fernández JM, et al. 2017. Genome-wide analysis of differential transcriptional and epigenetic variability across human immune cell types. *Genome Biol.* 18:18
27. Eng C-HL, Lawson M, Zhu Q, Dries R, Koulena N, et al. 2019. Transcriptome-scale super-resolved imaging in tissues by RNA seqFISH+. *Nature* 568:235–39
28. Fawkner-Corbett D, Antanaviciute A, Parikh K, Jagielowicz M, Gerós AS, et al. 2021. Spatiotemporal analysis of human intestinal development at single-cell resolution. *Cell* 184:810–26.e23
29. Floriddia EM, Lourenço T, Zhang S, van Bruggen D, Hilscher MM, et al. 2020. Distinct oligodendrocyte populations have spatial preference and different responses to spinal cord injury. *Nat. Commun.* 11:5860
30. Gaspar I, ed. 2018. *RNA Detection: Methods and Protocols*. New York: Springer
31. Gataric M, Park JS, Li T, Vaskivskyi V, Svedlund J, et al. 2021. PoSTcode: probabilistic image-based spatial transcriptomics decoder. bioRxiv 2021.10.12.464086. **https://doi.org/10.1101/2021.10.12.464086**
32. Gyllborg D, Langseth CM, Qian X, Choi E, Salas SM, et al. 2020. Hybridization-based in situ sequencing (HybISS) for spatially resolved transcriptomics in human and mouse brain tissue. *Nucleic Acids Res.* 48:e112

32a. Hao Y, Hao S, Andersen-Nissen E, Mauck WM, Zheng S, et al. 2021. Integrated analysis of multimodal single-cell data. *Cell* 184:3573–87.e29

33. Hagemann-Jensen M, Ziegenhain C, Chen P, Ramsköld D, Hendriks G-J, et al. 2020. Single-cell RNA counting at allele and isoform resolution using Smart-seq3. *Nat. Biotechnol.* 38:708–14
34. Hernández I, Qian X, Laláková J, Verheyen T, Hilscher M, Kühnemund M. 2019. Mapping brain cell types with CARTANA in situ sequencing on the Nikon Ti2-E microscope. *Nat. Methods.* **https://www.nature.com/articles/d42473-019-00264-8**

35. Hilscher MM, Gyllborg D, Yokota C, Nilsson M. 2020. In situ sequencing: a high-throughput, multi-targeted gene expression profiling technique for cell typing in tissue sections. *Methods Mol. Biol.* 2148:313–29
36. Hilscher MM, Langseth CM, Kukanja P, Yokota C, Nilsson M, Castelo-Branco G. 2022. Spatial and temporal heterogeneity in the lineage progression of fine oligodendrocyte subtypes. *BMC Biol*. 20:122
37. Jamal-Hanjani M, Wilson GA, McGranahan N, Birkbak NJ, Watkins TBK, et al. 2017. Tracking the evolution of non–small-cell lung cancer. *N. Engl. J. Med.* 376:2109–21
38. Janesick A, Shelansky R, Gottscho A, Wagner F, Rouault M, et al. 2022. High resolution mapping of the breast cancer tumor microenvironment using integrated single cell, spatial and in situ analysis of FFPE tissue. bioRxiv 2022.10.06.510405. **https://doi.org/10.1101/2022.10.06.510405**
39. Janosevic D, Myslinski J, McCarthy TW, Zollman A, Syed F, et al. 2021. The orchestrated cellular and molecular responses of the kidney to endotoxin define a precise sepsis timeline. *eLife* 10:e62270
40. Karran E, Mercken M, De Strooper B. 2011. The amyloid cascade hypothesis for Alzheimer's disease: an appraisal for the development of therapeutics. *Nat. Rev. Drug Discov.* 10:698–712
41. Ke R, Mignardi M, Pacureanu A, Svedlund J, Botling J, et al. 2013. In situ sequencing for RNA analysis in preserved tissue and cells. *Nat. Methods* 10:857–60
42. Krzywkowski T, Kühnemund M, Nilsson M. 2019. Chimeric padlock and iLock probes for increased efficiency of targeted RNA detection. *RNA* 25:82–89
43. La Manno G, Siletti K, Furlan A, Gyllborg D, Vinsland E, et al. 2021. Molecular architecture of the developing mouse brain. *Nature* 596:92–96
44. Landegren U, Kaiser R, Sanders J, Hood L. 1988. A ligase-mediated gene detection technique. *Science* 241:1077–80
45. Langseth CM, Gyllborg D, Miller JA, Close JL, Long B, et al. 2021. Comprehensive in situ mapping of human cortical transcriptomic cell types. *Commun. Biol.* 4:998
46. Laureyns R, Joossens J, Herwegh D, Pevernagie J, Pavie B, et al. 2022. An in situ sequencing approach maps PLASTOCHRON1 at the boundary between indeterminate and determinate cells. *Plant Physiol*. 188:782–94
47. Lee H, Salas SM, Gyllborg D, Nilsson M. 2022. Direct RNA targeted in situ sequencing for transcriptomic profiling in tissue. *Sci. Rep.* 12:7976
48. Lee JH, Daugharthy ER, Scheiman J, Kalhor R, Ferrante TC, et al. 2015. Fluorescent in situ sequencing (FISSEQ) of RNA for gene expression profiling in intact cells and tissues. *Nat. Protoc.* 10:442–58
49. Lee JH, Daugharthy ER, Scheiman J, Kalhor R, Yang JL, et al. 2014. Highly multiplexed subcellular RNA sequencing in situ. *Science* 343:1360–63
50. Lein E, Borm LE, Linnarsson S. 2017. The promise of spatial transcriptomics for neuroscience in the era of molecular cell typing. *Science* 358:64–69
51. Li X, Wang C-Y. 2021. From bulk, single-cell to spatial RNA sequencing. *Int. J. Oral Sci.* 13:36
52. Lindeboom RGH, Regev A, Teichmann SA. 2021. Towards a Human Cell Atlas: taking notes from the past. *Trends Genet.* 37:625–30
53. Liu I, Jiang L, Samuelsson ER, Salas SM, Beck A, et al. 2022. The landscape of tumor cell states and spatial organization in H3-K27M mutant diffuse midline glioma across age and location. *Nat. Genet.* 54:1881–94
54. Liu S, Punthambaker S, Iyer EPR, Ferrante T, Goodwin D, et al. 2021. Barcoded oligonucleotides ligated on RNA amplified for multiplexed and parallel in situ analyses. *Nucleic Acids Res*. 49:e58
55. Liu Y, Yang M, Deng Y, Su G, Enninful A, et al. 2020. High-spatial-resolution multi-omics sequencing via deterministic barcoding in tissue. *Cell* 183:1665–81.e18
56. Lomakin A, Svedlund J, Strell C, Gataric M, Shmatko A, et al. 2022. Spatial genomics maps the structure, nature and evolution of cancer clones. *Nature* 611:594–602
57. Lubeck E, Cai L. 2012. Single-cell systems biology by super-resolution imaging and combinatorial labeling. *Nat. Methods* 9:743–48
58. Luo J, Bergstrom DE, Barany F. 1996. Improving the fidelity of *Thermus thermophilus* DNA ligase. *Nucleic Acids Res*. 24:3071–78
59. Macosko EZ, Basu A, Satija R, Nemesh J, Shekhar K, et al. 2015. Highly parallel genome-wide expression profiling of individual cells using nanoliter droplets. *Cell* 161:1202–14

60. Magoulopoulou A, Qian X, Pediatama Setiabudiawan T, Salas SM, Yokota C, et al. 2022. Spatial resolution of *Mycobacterium tuberculosis* bacteria and their surrounding immune environments based on selected key transcripts in mouse lungs. *Front. Immunol.* 13:876321
60a. Mah CK, Ahmed N, Lam D, Monell A, Kern C, et al. 2022. Bento: a toolkit for subcellular analysis of spatial transcriptomics data. bioRxiv 2022.06.10.495510. **https://doi.org/10.1101/2022.06.10.495510**
61. Maley CC, Galipeau PC, Finley JC, Wongsurawat VJ, Li X, et al. 2006. Genetic clonal diversity predicts progression to esophageal adenocarcinoma. *Nat. Genet.* 38:468–73
62. Marshall JL, Noel T, Wang QS, Chen H, Murray E, et al. 2022. High-resolution Slide-seqV2 spatial transcriptomics enables discovery of disease-specific cell neighborhoods and pathways. *iScience* 25:104097
63. Marx V. 2021. Method of the Year: spatially resolved transcriptomics. *Nat. Methods* 18:9–14. Correction. 2021. *Nat. Methods* 18:219
64. McGranahan N, Swanton C. 2017. Clonal heterogeneity and tumor evolution: past, present, and the future. *Cell* 168:613–28
65. Moffitt JR, Hao J, Wang G, Chen KH, Babcock HP, Zhuang X. 2016. High-throughput single-cell gene-expression profiling with multiplexed error-robust fluorescence in situ hybridization. *PNAS* 113:11046–51
66. Muhlich JL, Chen Y-A, Yapp C, Russell D, Santagata S, Sorger PK. 2022. Stitching and registering highly multiplexed whole-slide images of tissues and tumors using ASHLAR. *Bioinformatics* 38:4613–21
67. *Nature*. 2021. Brain Initiative Cell Census Network. *Nature*. **https://www.nature.com/collections/cicghheddj**
68. Ngai J. 2022. BRAIN 2.0: transforming neuroscience. *Cell* 185:4–8
69. Nilsson M, Malmgren H, Samiotaki M, Kwiatkowski M, Chowdhary BP, Landegren U. 1994. Padlock probes: circularizing oligonucleotides for localized DNA detection. *Science* 265:2085–88
70. Nowell PC. 1976. The clonal evolution of tumor cell populations. *Science* 194:23–28
71. Ortiz C, Navarro JF, Jurek A, Märtin A, Lundeberg J, Meletis K. 2020. Molecular atlas of the adult mouse brain. *Sci. Adv.* 6:eabb3446
71a. Palla G, Spitzer H, Klein M, Fischer D, Schaar AC, et al. 2022. Squidpy: a scalable framework for spatial omics analysis. *Nat. Methods* 19:171–78
72. Park J, Choi W, Tiesmeyer S, Long B, Borm LE, et al. 2021. Cell segmentation-free inference of cell types from in situ transcriptomics data. *Nat. Commun.* 12:3545. Correction. 2021. *Nat. Commun.* 12:4103
73. Partel G, Hilscher MM, Milli G, Solorzano L, Klemm AH, et al. 2020. Automated identification of the mouse brain's spatial compartments from in situ sequencing data. *BMC Biol.* 18:144
74. Partel G, Wählby C. 2021. Graph-based image decoding for multiplexed in situ RNA detection. In *2020 25th International Conference on Pattern Recognition*, pp. 3783–90. Piscataway, NJ: IEEE
75. Partel G, Wählby C. 2021. Spage2vec: unsupervised representation of localized spatial gene expression signatures. *FEBS J.* 288:1859–70
76. Pelvig DP, Pakkenberg H, Stark AK, Pakkenberg B. 2008. Neocortical glial cell numbers in human brains. *Neurobiol. Aging* 29:1754–62
77. Petukhov V, Xu RJ, Soldatov RA, Cadinu P, Khodosevich K, et al. 2022. Cell segmentation in imaging-based spatial transcriptomics. *Nat. Biotechnol.* 40:345–54
78. Picelli S, Faridani OR, Björklund ÅK, Winberg G, Sagasser S, Sandberg R. 2014. Full-length RNA-seq from single cells using Smart-seq2. *Nat. Protoc.* 9:171–81
79. Qian X, Harris KD, Hauling T, Nicoloutsopoulos D, Muñoz-Manchado AB, et al. 2020. Probabilistic cell typing enables fine mapping of closely related cell types in situ. *Nat. Methods* 17:101–6
80. Regev A, Teichmann SA, Lander ES, Amit I, Benoist C, et al. 2017. The Human Cell Atlas. *eLife* 6:e27041
81. Rodriques SG, Stickels RR, Goeva A, Martin CA, Murray E, et al. 2019. Slide-seq: a scalable technology for measuring genome-wide expression at high spatial resolution. *Science* 363:1463–67
82. Roth R, Kim S, Kim J, Rhee S. 2020. Single-cell and spatial transcriptomics approaches of cardiovascular development and disease. *BMB Rep.* 53:393–99
83. Ruiz-Moreno C, Salas SM, Samuelsson E, Brandner S, Kranendonk MEG, et al. 2022. Harmonized single-cell landscape, intercellular crosstalk and tumor architecture of glioblastoma. bioRxiv 2022.08.27.505439. **https://doi.org/10.1101/2022.08.27.505439**

83a. Salas SM, Gyllborg D, Mattsson Langseth C, Nilsson M. 2021. Matisse: a MATLAB-based analysis toolbox for in situ sequencing expression maps. *BMC Bioinform.* 22:391
84. Sallinger K, Gruber M, Müller C-T, Bonstingl L, Pritz E, et al. 2022. Spatial tumour gene signature discriminates neoplastic from non-neoplastic compartments in colon cancer: unravelling predictive biomarkers for relapse. bioRxiv 2022.09.27.509641. **https://doi.org/10.1101/2022.09.27.509641**
84a. Satija R, Farrell JA, Gennert D, Schier AF, Regev A. 2015. Spatial reconstruction of single-cell gene expression data. *Nat. Biotechnol.* 33:495–502
85. Schmidt U, Weigert M, Broaddus C, Myers G. 2018. Cell detection with star-convex polygons. In *Medical Image Computing and Computer Assisted Intervention – MICCAI 2018*, ed. A Frangi, J Schnabel, C Davatzikos, C Alberola-López, G Fichtinger, pp. 265–73. Cham, Switz.: Springer
86. Shah S, Lubeck E, Schwarzkopf M, He T-F, Greenbaum A, et al. 2016. Single-molecule RNA detection at depth by hybridization chain reaction and tissue hydrogel embedding and clearing. *Development* 143:2862–67
86a. Singhal V, Chou N, Lee J, Liu J, Chock WK, et al. 2022. BANKSY: a spatial omics algorithm that unifies cell type clustering and tissue domain segmentation. bioRxiv 2022.04.14.488259. **https://doi.org/10.1101/2022.04.14.488259**
87. Soldatov R, Kaucka M, Kastriti ME, Petersen J, Chontorotzea T, et al. 2019. Spatiotemporal structure of cell fate decisions in murine neural crest. *Science* 364:eaas9536
88. Sountoulidis A, Liontos A, Nguyen HP, Firsova AB, Fysikopoulos A, et al. 2020. SCRINSHOT enables spatial mapping of cell states in tissue sections with single-cell resolution. *PLOS Biol.* 18:e3000675
89. Sountoulidis A, Salas SM, Braun E, Avenel C, Bergenstråhle J, et al. 2023. A topographic atlas defines developmental origins of cell heterogeneity in the human embryonic lung. *Nat. Cell Biol.* 25:351–65
90. Spelat R, Ferro F, Contessotto P, Aljaabary A, Martin-Saldaña S, et al. 2022. Metabolic reprogramming and membrane glycan remodeling as potential drivers of zebrafish heart regeneration. *Commun. Biol.* 5:1365
91. Ståhl PL, Salmén F, Vickovic S, Lundmark A, Navarro JF, et al. 2016. Visualization and analysis of gene expression in tissue sections by spatial transcriptomics. *Science* 353:78–82
92. Strell C, Hilscher MM, Laxman N, Svedlund J, Wu C, et al. 2019. Placing RNA in context and space – methods for spatially resolved transcriptomics. *FEBS J.* 286:1468–81
93. Stringer C, Wang T, Michaelos M, Pachitariu M. 2021. Cellpose: a generalist algorithm for cellular segmentation. *Nat. Methods* 18:100–106
94. Sun Y-C, Chen X, Fischer S, Lu S, Zhan H, et al. 2021. Integrating barcoded neuroanatomy with spatial transcriptional profiling enables identification of gene correlates of projections. *Nat. Neurosci.* 24:873–85
95. Svedlund J, Strell C, Qian X, Zilkens KJC, Tobin NP, et al. 2019. Generation of in situ sequencing based OncoMaps to spatially resolve gene expression profiles of diagnostic and prognostic markers in breast cancer. *EBioMedicine* 48:212–23
96. Tasic B, Yao Z, Graybuck LT, Smith KA, Nguyen TN, et al. 2018. Shared and distinct transcriptomic cell types across neocortical areas. *Nature* 563:72–78
97. Tiklová K, Björklund ÅK, Lahti L, Fiorenzano A, Nolbrant S, et al. 2019. Single-cell RNA sequencing reveals midbrain dopamine neuron diversity emerging during mouse brain development. *Nat. Commun.* 10:581
98. Tong J, Cao W, Barany F. 1999. Biochemical properties of a high fidelity DNA ligase from *Thermus* species AK16D. *Nucleic Acids Res.* 27:788–94
99. van Bruggen D, Pohl F, Langseth CM, Kukanja P, Lee H, et al. 2022. Developmental landscape of human forebrain at a single-cell level identifies early waves of oligodendrogenesis. *Dev. Cell* 57:1421–36.e5
100. Vickovic S, Eraslan G, Salmén F, Klughammer J, Stenbeck L, et al. 2019. High-definition spatial transcriptomics for in situ tissue profiling. *Nat. Methods* 16:987–90
101. Vickovic S, Schapiro D, Carlberg K, Lötstedt B, Larsson L, et al. 2022. Three-dimensional spatial transcriptomics uncovers cell type localizations in the human rheumatoid arthritis synovium. *Commun. Biol.* 5:129
102. Wang X, Allen WE, Wright MA, Sylwestrak EL, Samusik N, et al. 2018. Three-dimensional intact-tissue sequencing of single-cell transcriptional states. *Science* 361:eaat5691

103. Xia K, Sun H-X, Li J, Li J, Zhao Y, et al. 2022. The single-cell Stereo-seq reveals region-specific cell subtypes and transcriptome profiling in *Arabidopsis* leaves. *Dev. Cell* 57:1299–310.e4
104. Yates LR, Gerstung M, Knappskog S, Desmedt C, Gundem G, et al. 2015. Subclonal diversification of primary breast cancer revealed by multiregion sequencing. *Nat. Med.* 21:751–59
105. Yates LR, Knappskog S, Wedge D, Farmery JHR, Gonzalez S, et al. 2017. Genomic evolution of breast cancer metastasis and relapse. *Cancer Cell* 32:169–84.e7
106. Yuste R, Hawrylycz M, Aalling N, Aguilar-Valles A, Arendt D, et al. 2020. A community-based transcriptomics classification and nomenclature of neocortical cell types. *Nat. Neurosci.* 23:1456–68
107. Zeisel A, Hochgerner H, Lönnerberg P, Johnsson A, Memic F, et al. 2018. Molecular architecture of the mouse nervous system. *Cell* 174:999–1014.e22
108. Zheng Y, Zhong Y, Hu J, Shang X. 2021. SCC: an accurate imputation method for scRNA-seq dropouts based on a mixture model. *BMC Bioinform*. 22:5